

## IOX-101, a novel small molecule, reduces AML cell proliferation by Akt enzyme inhibition

Rajagopalan Prasanna<sup>1</sup>, Martin Raju<sup>2</sup>, Hateem Aseeri<sup>1</sup>, Ismail M Helal<sup>1,4</sup> and Ashraf A Elbessoumy<sup>1,3,\*</sup>

<sup>1</sup> Department of Clinical Laboratory Sciences, College of Applied Medical Sciences, King Khalid University, Abha, Kingdom of Saudi Arabia

<sup>2</sup> Department of Microbiology and Parasitology, College of Medicine, King Khalid University, Abha, Kingdom of Saudi Arabia

<sup>3</sup> Department of Biochemistry, Faculty of Science, Alexandria University, Alexandria, Egypt

<sup>4</sup> Plant Researches Department, Nuclear Research Center, Atomic Energy Authority, P. N. 13759, Egypt

\*Corresponding author: [absome@kku.edu.sa](mailto:absome@kku.edu.sa)

**Received:** September 22, 2017; **Revised:** November 1, 2017; **Accepted:** November 7, 2017; **Published online:** November 28, 2017

**Abstract:** Cancer of the blood continues to be a major mortality factor globally. Arylidene compounds are well known for their anticancer effects. Here we describe the biological efficacy of IOX-101, a potential lead-compound of arylidene in acute myeloid leukemia (AML). Initially, molecular docking analysis was performed to check the binding efficacy of the compound with protein kinase B (Akt). The ability of the molecule to inhibit AML proliferation was assessed in THP-1 and Kasumi-6 cells by a standard MTT assay. Hoechst 333258/propidium iodide (PI) staining was carried out to analyze the nuclear damage. Flow cytometry was performed to check the apoptotic and cell cycle changes in THP-1 cells. The effect of IOX-101 on Akt phosphorylation was assessed by Western blot analysis. Molecular docking revealed interaction and binding of IOX-101 with the active site of Akt enzyme. The compound reduced proliferation of both AML cell lines in a dose-responsive way. Nuclear staining and cell cycle results revealed DNA damage by IOX-101 in THP-1 cells, and a significant increase in early and late phase apoptotic cells. A dose-dependent dephosphorylation of Akt (Ser 473) by IOX-101 was observed, which indicated allosteric inhibition of Akt by the compound. Our results showed that the DNA damage-mediated antiproliferative effect of IOX-101 in AML cells was mediated by Akt enzyme inhibition, and that this molecule possesses an effective chemotherapeutic potential against AML.

**Key words:** Akt; acute myeloid leukemia (AML); apoptosis; cell cycle; IOX-101

## INTRODUCTION

AML accounts for the majority of hematological malignancies globally; unfortunately, it has not been met by a fully effective treatment [1]. This form of cancer is a stem cell-derived hematopoietic malignancy, characterized by uncontrolled proliferation and accumulation of myeloblasts in the bone marrow, blood and organs [2]. Current treatment regimens of AML are limited to combination chemotherapy and/or transplantation, thus leaving a wide field for the development of safe and efficacious drugs. As chemotherapeutics have dose limiting toxicities and the potential for acquired drug resistance, better and more effective chemotherapeutics with minimal adverse effects are needed to increase the patient survival rate [3].

Several studies have clearly linked phosphatidylinositol-4,5-bisphosphate 3-kinase (PI3K)/Akt signaling to with hematological malignancies, their development and progression [4-6]. Akt belongs to the serine/threonine kinase family, which participates in signal transduction that controls tumorigenesis and metastasis [7]. Compared to normal cells, Akt is significantly phosphorylated in malignant cells, where its activation helps in cancer cell survival. Thus, anomalies in Akt regulation drive it as a therapeutic intervention point for hematological malignancies, particularly in AML.

With increased understanding of medical biochemistry and biology at the molecular level, many synthetic compounds have been introduced for screening against cancers. Some of these compounds

have successfully emerged as effective, economical and less toxic drugs used to target different malignancies. Arylidene, with potential antitumor properties, belongs to this class of drug. We previously reported that an arylidene derivative (FXY-1) was effective against breast and lung cancer cells [8,9]. Based on these observations, we synthesized structural analogs of this compound by rational drug design and docked them with Akt to check the enzyme-compound affinity.

The current study focuses on one such compound, IOX-101, which exhibited a promising affinity towards Akt's active site that was screened against AML cells. The research also focused on the *in vitro* preclinical biological efficacy of the compound in AML.

## MATERIALS AND METHODS

### Materials

All chemicals and reagents were purchased from Sigma (Sigma, St. Louis, USA) unless otherwise indicated. THP-1 and Kasumi-6 cell lines were obtained from the American Type Culture Collection (ATCC). The Z'-LYTE kit was from Invitrogen Ltd (Invitrogen Thermo Fischer Scientific Inc, USA). The Annexin V kit was purchased from e-Bioscience Ltd., USA. The Cell Cycle reagent was obtained from Millipore Corp, USA. Akt and  $\beta$ -actin antibodies were purchased from Cell-Signaling, Santa Cruz, USA.

### Molecular modeling human Akt (huAkt)

To have a clean 3D-structure, we used MODELLER 9.14, which builds comparative models using the spatial restraint method [10]. Six models were generated, and the lowest energy conformer was selected for further processing. Further quality analysis of the model was performed using online tools such as RAMPAGE [11] and VERIFY-3D [12]. The finalized model was further energy minimized using GROMACS [13], with GROMOS96 54a7 force field [14]. IOX-101 structure was created with Chemsketch 14.01 [15]. We used AutoDockVina [16] for the docking analysis. Results were visualized and analyzed with PMV and LigPlot+ [17], respectively.

### Akt enzyme assay

Akt enzyme inhibition assay was carried out using Z'-LYTE™ (Invitrogen Ltd., USA) kit, a fluorescence-based, coupled enzyme format as per the manufacturer's instructions. The assay depends on the fluorescence resonance energy transfer (FRET) between a coumarin donor and fluorescein acceptor. The ratio of fluorescence emission at 520 nm to coumarin emission at 445 nm was used to quantify the reaction progress. Staurosporine was used as a positive control for the Akt inhibition assays.

### Cell culture

THP-1 and Kasumi -6 cells were grown in RPMI-1640 medium supplemented with 10% fetal bovine serum (FBS), 100 U/mL of penicillin and 100 U/mL of streptomycin. All cells (passage 3-12), were maintained in a humidified atmosphere at 5% CO<sub>2</sub> and 37°C. The medium was replaced every second day and maintenance was strictly in accordance with standard procedures.

### Cell proliferation assay

The proliferation assay was performed as described by Mosmann 1983 [18] with minor modifications. Five thousand cells/well in 100  $\mu$ L of RPMI media supplemented with 10% FBS and 1% penicillin and streptomycin were plated in triplicate in a 96-well plate. Cells were incubated overnight, and 50  $\mu$ L of IOX-101 at the desired final concentration was added along with a DMSO blank and incubated in appropriate conditions. Fifteen  $\mu$ L of 5 mg/mL 3-(4,5-dimethylthiazol-2-yl)-2,5-diphenyltetrazolium bromide (MTT) was added and incubated for 3.5 h. The medium was aspirated and MTT was dissolved in 150  $\mu$ L of dimethyl sulfoxide (DMSO) and absorbance was read at 560 nm with reference at 640 nm. Results were analyzed using GraphPad Prism software and are presented as the percentage of inhibition of cell proliferation.

### Morphological assay (dual staining)

Propidium iodide/Hoechst 333258 dual staining was performed as described [19] with slight modification. Briefly, THP-1 cells were incubated with 300 nM IOX-101 for 24 h and treated with 2  $\mu$ L of combined dye (100 mg/mL propidium iodide and 100 mg/mL

Hoechst 333258). Samples were transferred to a glass slide for immediate analysis using a fluorescence microscope (Nikon, Japan).

### Annexin V assay

The assay was performed using the annexin V detection kit from e-Biosciences, USA, as per the manufacturer's instructions as follows:  $0.5 \times 10^6$  THP-1 cells were treated with 300 nM or 600 nM IOX-101 and incubated in CO<sub>2</sub> incubator for 72 h; harvested cells were washed twice and incubated with 0.25 µg/mL annexin V reagent for 15 min; after several washes, the cells were resuspended in binding buffer containing 0.5 µg/mL PI and 10,000 events were acquired on a Guava easyCyte™ flow cytometer. Data were analyzed using InCyte software, Millipore. Early and late phase apoptotic cells were segregated with a quadruplet graph and the percentages of apoptotic cells were represented using GraphPad Prism software.

### Cell cycle analysis

THP-1 cells were seeded at a density of  $0.5 \times 10^6$  cells per well in a 6-well plate and incubated with IOX-101 at the desired concentrations for 72 h. Cells were stained with Guava® Cell Cycle reagent according to the manufacturer's instructions and 10000 events were acquired on a Guava easyCyte™ flow cytometer. Data were analyzed using Express Pro Software (Millipore, USA) and the percentage cell population in different cell cycle stages with respect to the control was calculated.

### Western immunoblotting

THP-1 cells ( $0.4 \times 10^6$ ) were plated in 2 mL of RPMI media supplemented with 10% FBS and 1% Pen-Strep in 6-well plates and incubated overnight. The next day, the medium was replaced with RPMI containing 0.04% FBS for 1 h, and the desired concentrations of IOX-101 were added along with a DMSO blank and incubated for 3 h. The cells were lysed, their total protein was determined using Bradford reagent and stored at -80°C. Equal amounts of protein were added to the loading buffer and denatured by boiling for 5 min. Samples were run on a 7.5% sodium dodecyl sulfate (SDS) gel, and then transferred onto a PVDF membrane. The membrane was blocked

with 5% bovine serum albumin (BSA) in TBS/0.1% Tween 20 for 1 h at room temperature on a shaker. The membrane was incubated with pAkt antibody overnight at 4°C. After washing, anti-rabbit IgG was added and kept at room temperature for 1 h. After 3 washes, the membranes were subjected to enhanced chemiluminescence (ECL). The blots were quantified by densitometry using ImageJ (Ver: 1.46, NIH) and normalized to actin. Results were plotted with GraphPad Prism 6 and analyzed for IC<sub>50</sub> values.

### Statistical analysis

All experiments were carried out in triplicate unless specified. The results are expressed as the mean±SE. Statistical analyses were performed using GraphPad Prism 6.0 (La Jolla, USA). IC<sub>50</sub> or GI<sub>50</sub> values were calculated using a nonlinear regression fit model with variable slope and plotted accordingly. Differences between two groups were analyzed using the two-tailed Student's t test and p<0.05(\*) or p<0.01(\*\*) were considered as statistically significant.

## RESULTS

### *In silico* docking revealed high affinity binding of IOX-101 to huAkt

In the first part of this study we examined the binding efficacy of IOX-101 with huAkt by *in silico* docking analysis. Results confirmed a high binding affinity of IOX-101 with the active site of the enzyme (Fig. 1B and C), with a docking energy of -9.2 kcal/mol. We further used LigPlot+ to determine the interacting residues of the enzyme with the compound. Fig. 1B shows interaction of IOX-101 with the active site of huAkt in the 150-408 amino acid region. Analyzing the Ligplot+ results, it was observed that maximal interaction energies were from hydrophobic interactions (the red crown indicates hydrophobic interactions).

### Inhibition of huAkt enzyme and decreased proliferation of AML cells

We next performed an *in vitro* assessment to evaluate the observed Akt enzyme inhibitory function of IOX-101. The kinase inhibitor staurosporine was used

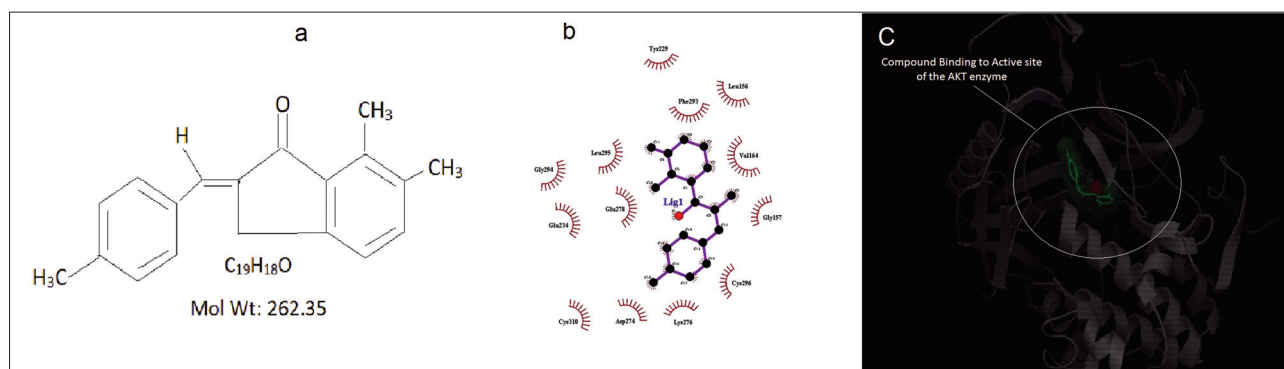


**Fig. 1.** IOX-101 to Akt *in silico* docking assessment . **A** – Chemical structure of IOX-101. **B** – LigPlot+ analysis depicting 2D interaction sites. Protein residues establishing ligand binding are shown as spokes around a black ball. Open spokes represent protein residues making non-bonding contacts with IOX-101. **C** – *In silico* docking analysis of compound binding to the active site of huAkt.

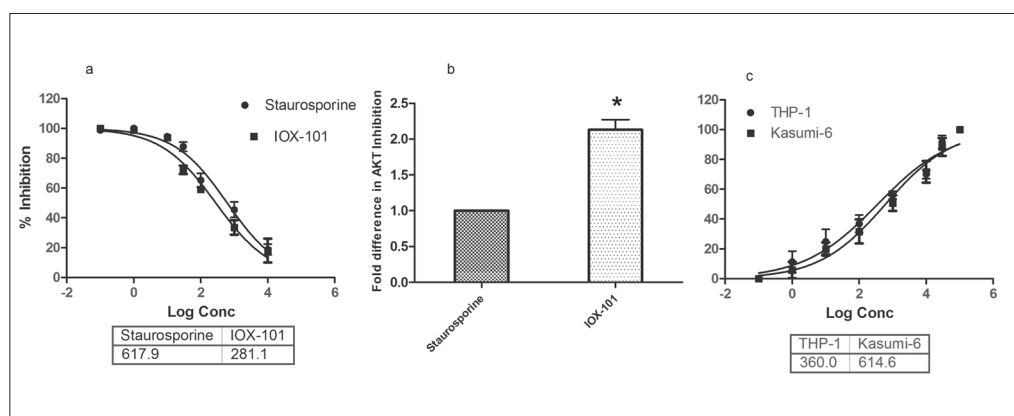


**Fig. 2.** Akt enzyme inhibition and antiproliferative profile of IOX-101. **A** – IC<sub>50</sub> of IOX-101 established by an Akt inhibition assay with staurosporine as a positive control. **B** – Fold inhibitory comparison of IOX-101 with the positive control. \* $p \leq 0.05$  compared to control **C** – Dose-dependent reduction in proliferation of THP-1 and Kasumi-6 AML cells by IOX-101. Conc – concentration.

as reference compound. It inhibited huAkt enzyme activity with an IC<sub>50</sub> of 281.1 nM (Fig 2A); the compound had more than double the efficacy in terms of Akt inhibition (Fig. 2B). Next, we investigated the antiproliferative effects of IOX-101 in different models of AML cells. The compound decreased the proliferation of both THP-1 and Kasumi-6 cells in a dose-dependent manner, with GI<sub>50</sub> of 360 nM and 614.1 nM, respectively (Fig. 2C). Because of higher efficacy and limited resources, further experiments were carried out with THP-1 cells.

### IOX-101 caused DNA damage and induced apoptosis in THP-1 cells

Based on the above results, we next investigated whether the antiproliferative effects were linked to

nuclear changes following compound addition to THP-1 cells. Staining with PI and Hoechst 333258 (Fig. 3A) revealed in THP-1 cells after IOX-101 treatment the presence of apoptotic bodies, characteristic cytoplasmic condensation/degradation and fragmented nuclei (Fig 3A.b), as compared to control cells (Fig 3A.a) whose nuclei remained intact. To substantiate the observed nuclear condensation effect with the apoptosis-inducing property of the drug, we carried out an annexin V assay in THP-1 cells after treatment with low and high doses of IOX-101. Flow cytometric observations of this assay revealed a dose-dependent increase in early and late phase apoptotic cells as compared to untreated cells (Fig. 3B). A significant dose-dependent increase in the total apoptotic percentage was observed in treated cells when compared with the control (Fig. 3C). To investigate the mechanism

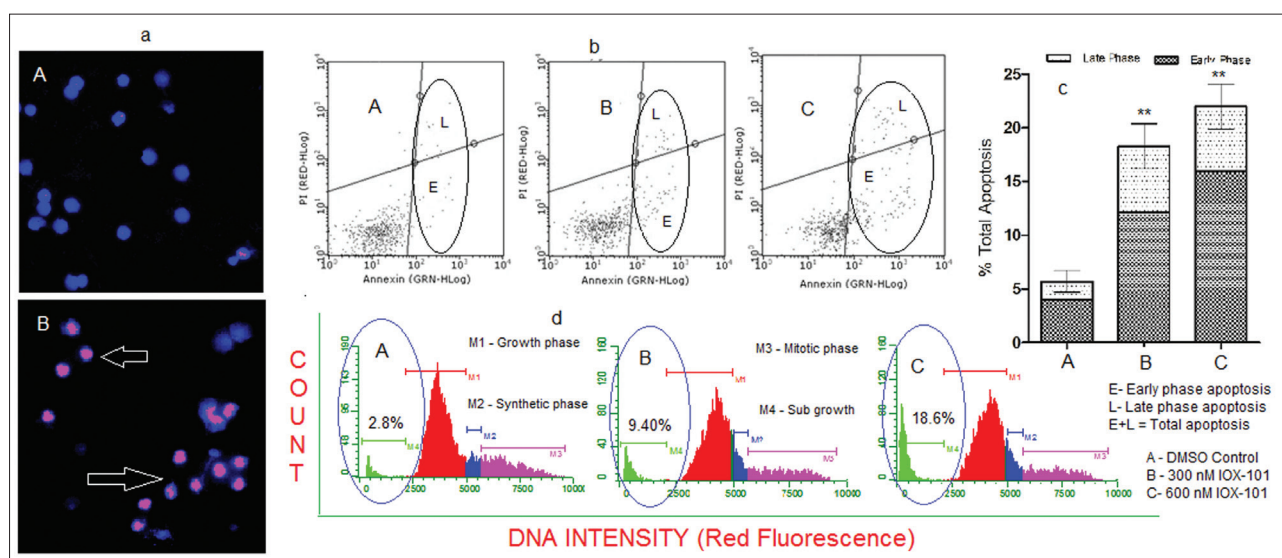


**Fig. 3.** Cellular effects of IOX-101 in AML cells. **A** – Hoechst/PI dual staining of THP-1 cells after IOX-101 treatment. Arrows show fragmented nuclei of THP-1 cells after treatment. **B** – Annexin V plots showing early and late phase apoptosis induction by IOX-101 in THP-1 cells. **C** – Increment of total apoptosis in THP-1 cells after treatment with IOX-101 in comparison with the control. Results are expressed as the mean±SD (\*\*Significant  $p \leq 0.01$ ). **D** – Cell cycle histograms of AML cells showing a dose-dependent increase in sub-growth phase cells after IOX-101 addition.

of apoptosis, in the next part of the study we evaluated the cell cycle changes after IOX-101 addition to THP-1 cells. As can be seen in Fig. 3D, treatment with 300 nM of the compound resulted in an increase in sub-growth phase ( $M_4$ ) cells to 9.4%, as compared to the DMSO-treated control, which had a corresponding 2.8% of cells in  $M_4$ . Increasing the concentration of IOX-101 to 600 nM resulted in an increase in  $M_4$  cells to 18.6% (Fig. 3D).

### Inactivation of Akt in AML cells by IOX-101

We examined the effect of IOX-101 on the dephosphorylation of Akt in THP-1 cells by Western blotting. The compound effectively suppressed pAkt (Ser 473) levels in THP-1 cells in a dose-responsive manner (Fig. 4A). The  $IC_{50}$  value was found to be 134.1 nM (Fig. 4B).

## DISCUSSION

Akt activation due to chromosomal translocation triggers permanent activation of an upstream tyrosine kinase in leukemic conditions [20]. Inhibition of mammalian target of rapamycin (mTOR) kinase, a downstream effector of Akt activation, leads to apop-

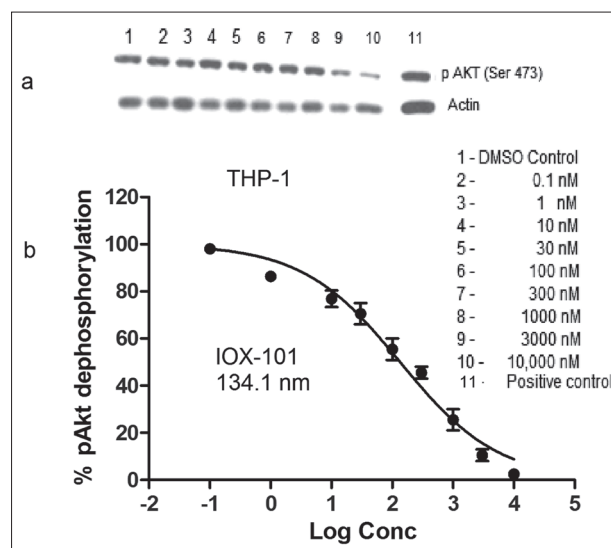


**Fig. 4.** Dephosphorylation of pAkt by IOX-101 in AML cells (**A**). Dose-dependent dephosphorylation of pAkt in THP-1 cells after IOX-101 treatment (**B**). Bands were quantified by densitometry using Image J (Ver: 1.46, NIH). After normalizing to actin, the results were plotted with GraphPad Prism 5 and analyzed for  $IC_{50}$  values from three individual experiments performed in duplicate. Conc – concentration.

to- sis of cells originating from both B- and T-cells in acute leukemia patients [21]. The above study presents the Akt pathway as an attractive target for drug development and treatment of a wide variety of he-

matological malignancies. Arylidene derivatives are bioactive compounds and studies have described their antiproliferative effects in cancerous cell lines [22]. Our prior experience with arylidene derivatives and their promising activities allowed us to establish a structure-activity relationship between IOX-101 and analogs of compound FXY-1 [9]. In the current study, we performed an *in-silico* docking analysis to establish whether our synthesized analogs have the potential to inhibit huAkt. Akt has two potential binding cavities, including a pleckstrin homology domain (PH domain) that targets various phosphatidylinositols lying between 150-408 amino acid residues [23]. Our result suggests that IOX-101 has a high affinity for this site, with a binding energy of -9.2 k-cal/mol. This clear-cut interaction at the active site is in agreement with previously established procedures used to explain the compound's efficacy in enzyme inhibition [24].

Uncontrolled cell proliferation is a major event of disease progression in acute leukemia and Akt plays an important cellular role in controlling proliferation. Studies have clearly established that Akt inhibition, either by siRNA or an inhibitor, results in reduced cancer cell proliferation [25]. Our results on huAkt inhibition and the dose-dependent reduction of proliferation by IOX-101 in two models of AML proves that the compound's antiproliferative effects in AML are the result of Akt inhibition.

We next examined the nuclear status of the THP-1 cells after treatment with IOX-101. The observed morphological changes, including nuclear condensation/fragmentation observed after PI and Hoechst 333258 staining, suggested common apoptotic events, and were in accordance with literature data [26,27]. As an early event in the apoptotic process, phosphatidyl serine (PS) translocates from the inner side of the plasma membrane to the outer surface. Annexin V binds with high affinity to the PS and clearly delineates early and late phases of apoptosis [28]. Our observation of dose-dependent early, late and total apoptosis after IOX-101 treatment of THP-1 cells supports the assumption that apoptotic events are responsible for the observed antiproliferative effects of the compound.

Cell cycle regulation remains as an important event in deciding between survival and death, particularly in the treatment regimen of cancer cells. One

of the hallmarks of apoptosis is the genomic DNA digestion by endonuclease whereby the cellular DNA content is reduced [28]. In the current study, the occurrence of a hypodiploid peak after staining with DNA-specific fluorescent dyes helped in identifying the IOX-101-induced apoptotic mode of cell death in AML cells. The rise in this  $M_4$  peak observed after cycle analysis was due to a reduction in DNA content caused by IOX-101 treatment, and was in line with the morphological observations of dual staining.

Phosphorylation of Akt triggers a number of downstream signals that are required for cancer cell survival [29]. To substantiate the detected Akt inhibition by IOX-101, we investigated the role of pAkt expression in AML cells. Our results showed down-regulation of endogenous Akt (Ser 473) phosphorylation in THP-1 cells, suggesting that IOX-101 induced apoptosis in AML cells that was brought about by dephosphorylation of the kinase.

## CONCLUSION

In a model of AML cells, this study reveals the excellent antiproliferative effects of IOX-101 caused by Akt inhibition. Further research on animal models is necessary to take this molecule to the next level of preclinical studies and further develop it as an effective chemotherapeutic against AML.

**Acknowledgments:** The authors are grateful to the Deanship of Scientific Research, King Khalid University, Abha, K.S.A. for funding the work (Project Number 110)

**Author contributions:** All authors contributed towards the design, work and analysis presented in the current study.

**Conflict of interest disclosure:** The authors hereby declare no conflict of interest related to this study.

## REFERENCES

1. Ramos NR, Mo CC, Karp JE, Hourigan CS. Current Approaches in the Treatment of Relapsed and Refractory Acute Myeloid Leukemia. *J Clin Med.* 2015;4(4):665-95.
2. Herrmann H, Blatt K, Shi J, Gleixner KV, Cerny-Reiterer S, Müllauer L, Vakoc CR, Sperr WR, Horny HP, Bradner JE, Zuber J, Valent P. Small-molecule inhibition of BRD4 as a new potent approach to eliminate leukemic stem- and progenitor cells in acute myeloid leukemia (AML). *Oncotarget.* 2012;3:1588-99.

3. Mateen S, Tyagi A, Agarwal C, Singh RP, Agarwal R. Silibinin inhibits human nonsmall cell lung cancer cell growth through cell-cycle arrest by modulating expression and function of key cell-cycle regulators. *Mol Carcinog*. 2010;49(3):247-58
4. Hennessy BT, Smith DL, Ram PT, Lu Y, Mills GB. Exploiting the PI3K/AKT pathway for cancer drug discovery. *Nat Rev Drug Discov*. 2005;4:988-04.
5. Shaw RJ, Cantley LC. Ras, PI(3)K and mTOR signaling controls tumour cell growth. *Nature*. 2006;441:424-30.
6. Witzig TE, Kaufmann SH. Inhibition of the phosphatidylinositol 3-kinase/mammalian target of rapamycin pathway in hematologic malignancies. *Curr Treat Options Oncol*. 2006;7:285-94.
7. Fong Y, Lin YC, Wu CY, Wang HM, Lin LL, Chou HL, Teng YN, Yuan SS, Chiu CC. The Antiproliferative and Apoptotic Effects of Sirtinol, a Sirtuin Inhibitor on Human Lung Cancer Cells by Modulating Akt/ $\beta$ -Catenin-Foxo3A Axis. *Scientific-WorldJournal*. 2014;2014:937051.
8. Prasanna R, Harish CC. Anticancer Effect of a Novel 2-Arylidene-4,7-dimethyl indan-1-one Against Human Breast Adenocarcinoma Cell Line by G2/M Cell Cycle Arrest. *Oncol Res*. 2010;18(10):461-8.
9. Rajagopalan Prasanna, Alahmari KA, Elbessoumy AA, Balasubramaniam M, Suresh R, Shariff ME, Chandramoorthy HC. Biological evaluation of 2-arylidene-4, 7-dimethyl indan-1-one (FXY-1): a novel Akt inhibitor with potent activity in lung cancer. *Cancer Chemother Pharmacol*. 2016;77(2):393-04.
10. Eswar N, Marti-Renom MA, Webb B, Madhusudhan MS, Eramian D, Shen M, Pieper U, Sali A. Comparative Protein Structure Modeling With MODELLER. *Curr Protoc Protein Sci*. 2006;05:5:5-6.
11. Lovell SC, Davis IW, Arendall III WB, de Bakker PIW, Word JM, Prisant MG, Richardson JC, Richardson DC. Structure validation by C $\alpha$  geometry: phi,psi and C $\beta$  deviation. *Proteins*. 2002;50:437-50.
12. Luthy R, Bowie JU, Eisenberg D. Assessment of protein models with three-dimensional profiles. *Nature*. 1992;356(6364):83-5.
13. Berendsen HJC, van der Spoel D, van Drunen R. GROMACS: a message-passing parallel molecular dynamics implementation. *Comput Phys Commun*. 1995. 91:43-56.
14. Nathan Schmid, Andreas P, Eichenberger, Alexandra Choutko, Sereina Riniker, Moritz Winger, Alan E. Mark, Wilfred F, van Gunsteren. Definition and testing of the GROMOS force-field versions 54A7 and 54B7. *Eur Biophys J*. 2011;40:843-56.
15. Chemskech [Internet]. Version 14.01. Toronto ON, Canada: Advanced Chemistry Department. 2014- [Updated November 2017, cited 2014 May 01]. Available from :<http://www.acdlabs.com>
16. Morris GM, Huey R, Lindstrom W, Sanner MF, Belew RK, Goodsell DS, Olson AJ. Autodock4 and AutoDockTools4: automated docking with selective receptor flexibility. *J Computational Chemistry*. 2009;16:2785-91.
17. Laskowski R A, Swindells M B. LigPlot+: multiple ligand-protein interaction diagrams for drug discovery. *J Chem Inf*. 2011;51: 2778-86.
18. Mosmann T. Rapid colorimetric assay for cellular growth and survival: application to proliferation and cytotoxicity assays. *J Immunol Methods*. 1983;65:55-63.
19. Belloc F, Dumain P, Boisseau MR, Jalloustre C, Reiffers J, Bernard P. A flow cytometric method using Hoechst 33342 and propidium iodide for simultaneous cell cycle analysis and apoptosis determination in unfixed cells. *Cytometry*. 1994;17:59-65.
20. Skorski T, Bellacosa A, Nieborowska-Skorska M, Majewski M, Martinez R, Choi JK, Trotta R, Wlodarski P, Perrotti D, Chan TO, Wasik MA, Tsichlis PN, Calabretta B. Transformation of hematopoietic cells by BCR/ABL requires activation of a PI-3k/Akt-dependent pathway. *EMBO J*. 1997;16:6151-61.
21. Avellino R, Romano S, Parasole R, Bisogni R, Lamberti A, Poggi V, Venuta S, Romano MF. Rapamycin stimulates apoptosis of childhood acute lymphoblastic leukemia cells. *Blood*. 2005;106:1400-6.
22. Mahavir C, Anil Kumar S, Vijay T. Synthesis of 5-arylidene amino-1,3,4-thiadiazol-2-[(N-substituted benzylo)]sulphonamides endowed with potent antioxidants and anticancer activity induces growth inhibition in HEK293, BT474 and NCI-H226 cells. *Med Chem Res*. 2014;23(6):3049-64.
23. Knighton DR, Zheng JH, Ten Eyck LF, Ashford VA, Xuong NH, Taylor SS, Sowadski JM. Crystal structure of the catalytic subunit of cyclic adenosine monophosphate-dependent protein kinase. *Science*. 1991;26:407-14.
24. Zeng P, Liu B, Wang Q, Fan Q, Diao JX, Tang J, Fu XQ, Sun XG. Apigenin Attenuates Atherogenesis through Inducing Macrophage Apoptosis via Inhibition of AKT Ser473 Phosphorylation and Downregulation of Plasminogen Activator Inhibitor-2. *Oxid Med Cell Longev*. 2015;2015:379538.
25. Zhang BG, Du T, Zang MD, Chang Q, Fan ZY3, Li JF, Yu BQ, Su LP, Li C, Yan C, Gu QL, Zhu ZG, Yan M, Liu B. Androgen receptor promotes gastric cancer cell migration and invasion via AKT-phosphorylation dependent upregulation of matrix metalloproteinase 9. *Oncotarget*. 2014;5(21):10584-95.
26. Searle J, Lawson TA, Abbott PJ, Harmon B, Kerr JFR. An electron-microscope study of the mode of cell death induced by cancer chemotherapeutic agents in populations of proliferating normal and neoplastic cells. *J Pathol* 1994;116:129-38.
27. Hsu SL, Yin SC, Liu MC, Reichert U, Ho WL. Involvement of cyclin-dependent kinase activities in CD437-induced apoptosis. *Exp Cell Res*. 1999;252(2):332-41
28. Yoshihiro Higuchi. Glutathione depletion – induced chromosomal DNA \ fragmentation associated with apoptosis and necrosis. *J Cell Mol Med*. 2004;18(4):445-64.
29. Tanel A, Averill-Bates DA. P38 and ERK mitogen-activated protein kinases mediate acrolein-induced apoptosis in Chinese hamster ovary cells. *Cell Signal*. 2007;19(5):968-77.